Artificial Neural Networks-Based Radar Remote Sensing to Estimate Geographical Information during Oil-Spills

Bilal Hammoud
Technical University of Kaiserslautern
Kaiserslautern, Germany
hammoud@eit.uni-kl.de

Charbel Bou Maroun
Lebanese American University
Byblos, Lebanon
charbel.boumaroun01@lau.edu

Jonas Ney
Technical University of Kaiserslautern
Kaiserslautern, Germany
ney@eit.uni-kl.de

Norbert Wehn
Technical University of Kaiserslautern
Kaiserslautern, Germany
wehn@eit.uni-kl.de

***Abstract*—In this paper, we demonstrate how an artificial neural network (ANN) of low complexity can be used on radar data in the remote sensing field to estimate geographical information from oil-spills scenes. The work aims at the extraction of two features that are important for an effective contingency plan: the thickness of thick oil slicks, and their relative dielectric constant physical parameter. The adopted system model assumes reflectivities measured by wide-band radar sensors operating in C- and X- frequency bands and mounted on nadir-looking systems such as drones. It extracts the thickness of oil slicks being in the $1-10$ millimeter range and the dimensionless relative dielectric constant (permittivity) of the heavy oil material in the $2.8-3.3$ range. We test the accuracy of the ANN model using simulated and in-lab experimental data. Finally, we validate the low complexity of our approach by providing FPGA implementation results of the inference. To the best of our knowledge, ANNs in combination with the active radar sensor have not been used for oil-spills parameters' estimation so far.**

***Index Terms*—oil spill, radar reflectivity, artificial neural network, estimation, slicks' thickness, relative permittivity.**

I. Introduction

Environmental damage to marine life due to oil spills might last for years. After locating oil slicks, successful monitoring necessitates the estimation of geographical parameters so that proper measures are taken in tactical and strategic responses. The first parameter which is of great importance is the thickness of oil slicks [1]. This information is very helpful for spill-containment because it gives an indication about the total volume spilled. Another important task to perform during oil-spills is to specify the oil type to predict the environmental damage on the maritime life [2]. This information can be analyzed from the physical characteristics of the oil material, namely the relative dielectric constant (also called permittivity) [3]. While visual techniques that are based on slicks' appearance are not reliable due to light interference, state-of-the-art technologies for oil spill surveillance include the use of multiple sensors [4]. Although infrared sensors can be used for spill detection, the variation in the slick thickness does not affect the brightness of the infrared imagery [5] which makes these sensors not suitable for thickness estimation. Laser-acoustic sensors are reported to measure 6 mm slicks [6], but they cannot work under all weather conditions, require a dedicated aircraft, and they are expensive and bulky [7]. Alternatively, passive microwave radiometry sensors show potential for thickness estimations, but commercial instruments provide estimations for limited ranges only, up to 3 mm as reported in [8]. Recent studies used machine learning approaches to tackle the thickness estimation [9] where convolutional neural network are applied on hyperspectral images obtained using drones to detect oil slicks with different thicknesses up to 3.5 mm. Overall, few reliable methods capable of accurately measuring the thickness of the oil on top of the sea surface have been advanced [4].

For oil classification, chemical methods or laser fluorometric spectra can provide oil types [10], [11], but they require in-situ sampling and are not adequate for fast intervention. Recent machine learning algorithms are developed to overcome this limitation by remotely classifying oil slicks using hyperspectral sensors [12] and synthetic aperture radar [13]. Yet, to the best of our knowledge, no previous research has tackled the problem of estimating at the same time (1) the physical characteristics of the oil slicks and (2) their thicknesses within the full range from 1 to 10 mm using classical or machine learning algorithms applied on radar data.

Previously, we targeted the thickness estimation by applying an iterative procedure on measured reflectivities [14], maximum likelihood algorithms [15], [16], and a support vector regression model [17]. In this paper, we demonstrate how a simple low-power low-complexity artificial neural network (ANN)-based model can be used to not only accurately estimate the thickness of oil slicks, but also to estimate their relative permittivity for different oil-types classification.

II. System Model

A. Radar Reflectivity

At the system-level, the radar operates as a nadir-looking system to allow the full capture of the reflectivity without losses due to off-nadir back-scattering. To physically model the oil slicks on top of the sea surface, we consider a multi-layer structure (air, oil, and sea water) where each layer has its own electrical properties and physical characteristics. The latter determine the behavior of the electromagnetic (EM) field at the boundaries of the different dielectric media which are assumed to be nonmagnetic. Each medium in the multi-layer structure is characterized by its relative dielectric constant physical property ε_i for $i \in \{1, 2, 3\}$. We denote ε_1, ε_2, ε_3 to be corresponding to the air, oil, and sea water layer, respectively. The reflection (ρ) coefficients for the different interfaces (air-oil, and oil-water) are calculated respectively using:

$$\rho_{ij}(\varepsilon_i, \varepsilon_j) = \frac{\sqrt{\varepsilon_i} - \sqrt{\varepsilon_j}}{\sqrt{\varepsilon_i} + \sqrt{\varepsilon_j}} \tag{1}$$

Across the boundaries of the different layers, where the interaction with EM waves occurs, the electric field E is conserved. Let E_i^+, and E_i^-, be the electric fields in the medium i propagating towards to, and away from, the boundary interface to another medium j, respectively. The propagation of EM waves across the first interface between the air and the oil layer is captured by (1). However, the propagation through the second layer (oil) in the multi-layer structure will introduce a phase shift δ which is dependent on the oil relative dielectric constant ε_2, the frequency of the transmitted electromagnetic wave f_k (we keep the sub-index k for consistency with the following sections), and the thickness of the oil slick d. It is given by:

$$\delta(f_k, \sqrt{\varepsilon_2}, d) = \frac{2\,\pi\, f_k\, \sqrt{\varepsilon_2}\, d}{c} \tag{2}$$

where c is the speed of light. We can derive the reflectivity (power reflection coefficient) for the three-layer structure, as in [18], to get:

$$\underset{i\in\{1,2,3\}}{R(f_k, \varepsilon_i, d)} = \left|\frac{E_1^-}{E_1^+}\right|^2 = \frac{\rho_{12}^2 + \rho_{23}^2 + 2\,\rho_{12}\,\rho_{23}\,\cos(2\,\delta)}{1 + \rho_{12}^2\,\rho_{23}^2 + 2\,\rho_{12}\,\rho_{23}\,\cos(2\,\delta)} \tag{3}$$

The reflectivity R is a trigonometric function with period T_R that is dependent on the oil-refractive index and the frequency of the electromagnetic wave. The period is expressed as:

$$T_R(f_k, \varepsilon_2) = \frac{c}{2\, f_k\, \sqrt{\varepsilon_2}} \tag{4}$$

B. Oil-on-Ocean Surface Roughness

Two statistical attributes are of special importance to describe the roughness of ocean surface: (1) the rms-height (denoted by s) and (2) the surface correlation length which measures how much the surfaces at different locations are statistically correlated. Since we are interested in the surface parameters that are relevant to the wavelength of EM waves, we define for a surface its electromagnetic roughness ks [19] to be:

$$ks = 2\pi\, f_k\, s \tag{5}$$

Then, the scattering pattern will also include a non-coherent component along all other directions. In that case, the reflectivity along the specular direction will be noted as the coherent reflectivity (R_{coh}) [19], expressed as:

$$R_{coh} = R\, e^{-4(ks\,\cos(\theta_i))^2} \tag{6}$$

with θ_i being the incident angle of the EM wave to the interfaces. When considering thick oil slicks, the thickness is in the mm range. Such a thick layer dampens the ocean waves and reduces the roughness of the surfaceIn open ocean space and at very low wind speeds, the correlation length of the ocean waves is large and the root mean square height of the capillary waves is small. Hence, the effect of the oil layer under calm ocean conditions is to smooth the sea surface roughness [20] which is a consequence of practical importance for oil-spill scene's analysis. Hence, without loss of generality, all interfaces in the following are assumed smoothed within the radar cross section.

III. Estimation Model

A. Features Selection

The reflectivity shown in (3) involves the altered features of the sea surface by the covering oil slick. It is dependent on the physical properties of the multi-layer structure (ε_i), the frequency of the transmitted EM (f_k), and the thickness of the intermediate layer (d). Since the selection of transmitted EM wave is a parameter that is controlled by the operator on-site, and the physical properties of the air and water can be easily calculated, then, post-processing the radar reflectivity values will allow to extract the implicit information about the thickness and the relative permittivity of the thick oil layer covering the sea surface. Fig. 1 shows the theoretical reflectivities evaluated at different frequencies (4, 8, and 12 GHz) and different relative permittivities (2.8, 3, 3.3) for thicknesses of the oil slick in the ($1-10$ mm) range. For the same frequency, the effect of the variation in the relative permittivity on the reflectivity value is really dependent on the oil thickness. For instance, at f = 4 GHz (blue plots) the reflectivity value is almost the same between 1 and 4 mm even if the permittivity varies between 2.8 and 3.3. But, the reflectivity drops by more than 1 dB for different permittivities when the oil thickness is 10 mm. Similarly, at f = 12 GHz (red plots), the reflectivity drops by more than 1 dB due to the permittivity variation within thickness ranges ($2.5-3.5$) and ($8.5-10$) mm, whereas it varies slightly between 4 and 7 mm. Also, by looking at the reflectivity plots at the same frequency, they look very similar over the full thickness range even if the relative permittivity of the oil slick is changing. However, the reflectivity behavior varies a lot from one frequency to another. For instance, at 4 GHz, the curve of the reflectivity is monotonically decreasing slowly with the thickness. Hence, for small thickness values, the difference between the reflectivity values is very small, so the estimation could go easily wrong. A different pattern is observed at higher frequencies (8 or 12 GHz). The reflectivity curves admit a steeper slope for small values of thicknesses which improves the

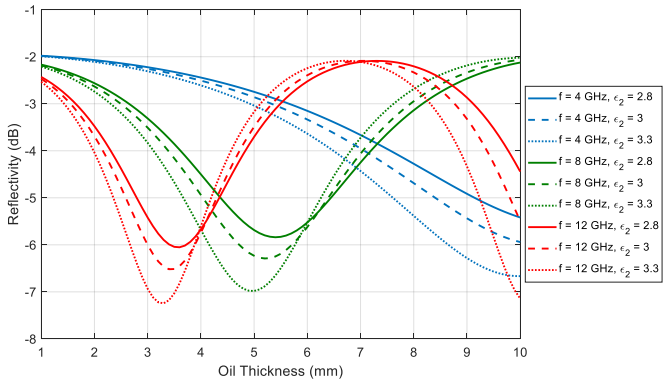

Fig. 1: Theoretical reflectivities evaluated at different frequencies (4, 8, 12 GHz), oil thicknesses (1−10 mm), and oil relative permittivities (2.8, 3, 3.3).

estimation of oil slick thickness. However, the cyclic behavior due to the periodicity of the reflectivity shown in 4 appears clearly within the targeted thickness range (1−10 mm) for 8 or 12 GHz frequencies. Hence, using higher frequencies introduces ambiguity in the estimation since many thicknesses can give the same reflectivity value. This highlights the need to process at a time multiple reflectivities evaluated at different frequencies in order to provide distinctive reflectivities for each oil thickness and permittivity. In our model, we will use 9 frequencies selected uniformly from C- (4−8 GHz) and X- (8−12 GHz) bands. Therefore, the input features to the model will be reflectivities evaluated at $f_k \in \{4{:}1{:}12\}$ GHz.

B. Neural Network Model

The machine learning model is a Regression ANN. Based on a set of inputs, the ANN model is designed to predict two output parameters as continuous quantities: the thickness of oil slicks, and the relative dielectric constant. The selection of the ANN and not other regression algorithms is due its ability to handle complexity. Our problem is to extract the thickness and permittivity of an oil spill using several sampled reflectivities, our inputs and outputs have a highly nonlinear relationship. In addition to that, ANNs benefit greatly from large amount of data, which we have at our disposal. Concerning the architecture of our model, we have decided to go with 3 hidden layers with respectively 12, 16 and 12 neurons in each layer. The activation function used on these layers is the rectified linear activation function (ReLU). We came up with this simple architecture after carefully studying the complexity of our problem and through trial and error. In our case, having more layers and neurons would lead to overfitting, and having less of them would prevent the model from encapsulating the relationship between our inputs and outputs. For the remaining hyperparameters, we are using the mean square error lost function and the "Adam" optimizer with a learning rate of 0.001, which are typically used for regression problems.

C. Training Process

Monte Carlo simulations are performed in MATLAB to generate the training data. The dielectric constant of the air is $\varepsilon_1 = 1$. The dielectric constant of the thick oil ε_2 is assumed to be real and selected from $\{2.8{:}0.1{:}3.3\}$. For the calculation of sea water dielectric constant, ε_3, we used the water temperature t_w as 20 °C, and the water salinity s_w as 35 ppt. We consider calm ocean conditions to capture the full reflectivity from the multi-layer structure by normal incidence of the EM waves. The noise in the system is considered to be additive white Gaussian (AWGN), with variance of $\sigma^2 = 0.001$. 10000 data points are generated for every integer thickness value in (1−10 mm) and every permittivity value in 2.8:1:3.3, making the overall number of data points to be 600000. The simulated data is used to train the NN model. 80% of the simulated data are used for training and the remaining 20% are used for testing and validation.

D. Multiple Observations

To further improve our model's accuracy, we also incorporate multiple observations to boost our estimator's performance. For N observations evaluated at each frequency, the average of N reflectivities is passed as an input feature to the NN model. This approach targets the reduction of the AWGN's effect on the accuracy of the estimations. This averaging step will be tested on the experimental data whereas a single observation approach will be used for the testing on simulation data.

IV. Simulation Results

Fig. 2 shows the predicted thicknesses (y-axis) versus the actual tested ones (x-axis). For better visualizing the results, the red line represents the ideal estimations when no error occurs. The blue points are the estimations spanning over ± one standard deviation around their mean. From the obtained results, the predicted thicknesses are accurate to the ± 0.5 mm in most cases. The error decreases when testing on integer thickness values, and increases slightly when testing is performed on fractional values. This is a great advantage of the model because, even though the training is done based on integer values for thicknesses, when testing the model on more realistic thickness values which are fractional, the deviation in the estimation is still small. Although the reflectivity shows cyclic behavior with respect to the thickness, the ANN model can explore their dependence over the full plausible range by jointly analyzing the reflectivity behavior at multiple frequencies. Therefore, as seen in fig. 2, the distribution of the estimations does not show a high error value. For instance, testing the model at 5.5 mm would still lead to estimations between 5 and 6.1 mm.

Similarly, fig. 3 shows the predicted relative permittivity (y-axis) versus the actual value (x-axis). The vertical blue bars represent the distribution of estimated values around the mean, marked by "x". Relative permittivity values 2.9, 3, and 3.1 are approximated accurately where the shift in estimations' mean is smaller than 0.05. The error in estimations for the remaining values 2.8, 3.2, and 3.3 is higher. Fig. 2 and 3

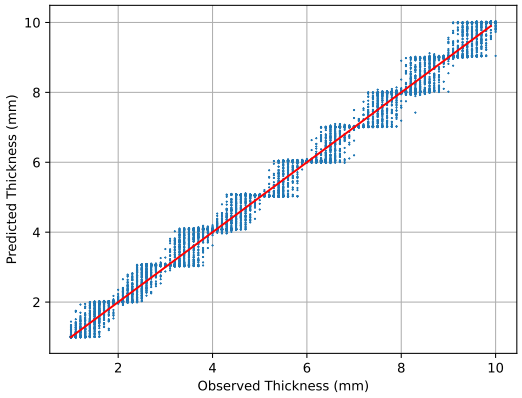

Fig. 2: Predicted thicknesses (y-axis) versus the actual values (x-axis). The blue points are the estimations span over $\pm$ one standard deviation around their mean.

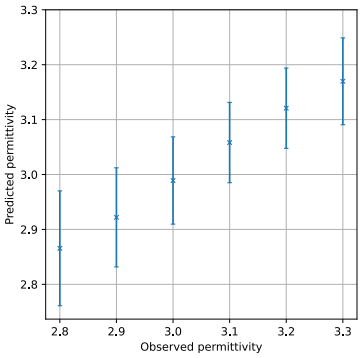

Fig. 3: Error bars of predicted relative permittivity (y-axis) versus the actual value (x-axis). x represents the mean of the estimations.

clearly show that the ANN model can extract the geographical parameters (thickness and relative permittivity of oil slicks) from the collected multi-frequency reflectivity values within an acceptable margin of error.

During an actual oil spill, slicks that are closer to the source of spill are characterized by higher thicknesses. The thickness gets gradually less thick going outwards of the initial spill point. We replicate this specific scenario in a simulation using the simulated reflectivities for thickness values ranging from 1 mm to 10 mm when the relative permittivity of the oil material is 3. Results are displayed in fig. 4. The center of the spill has the thickest thickness of 10 mm (dark brown) which decreases uniformly to 1 mm (dark blue). At the top left, we see the actual scenario. At the top right, the reconstruction of the environment made by the trained ANN model is presented. Similarly, the map at the bottom shows the estimations of the relative dielectric constant for the oil slicks. Obtained maps validate the accuracy of the model presented previously. The overall layout of the oil spill is correctly detected, even with

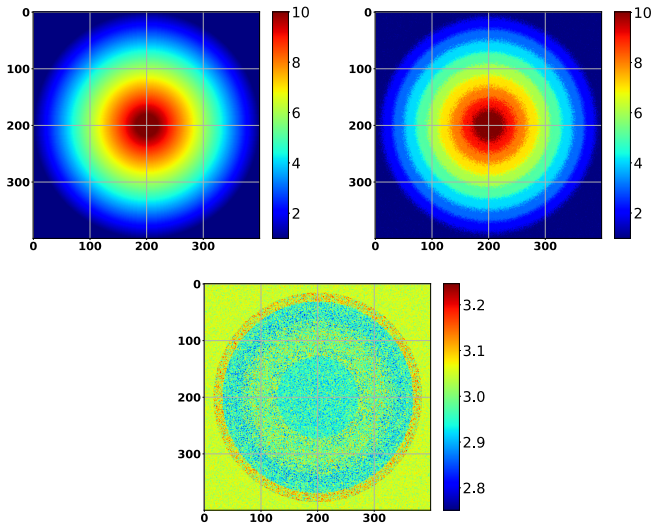

Fig. 4: (Left) Actual thickness distribution of an oil spill simulated scenario. (Right) Estimated thickness distribution obtained by the ANN model. (Bottom) Estimated relative permittivity distribution obtained by the ANN model.

some errors in the model's estimations, most of the errors fall around $\pm$ 1 mm of the actual thickness indicating that our model would be valid a similar scenario of an actual oil spill. The average estimation for the relative permittivity over the full map is 3.03, which is very accurately predicting the actual value. Since our approach is supposed to be used in real scenarios, we validate its performance by applying it on in-lab experimental data in the next section.

V. Experimental Results

We use radar reflectivity measurements from an oil-spill in-lab experiment detailed in [21]. The two parameters' estimation is performed on experimental reflectivities measured at 9 selected frequencies (4.38, 5.37, 5.99, 6.97, 7.98, 9.06, 10.14, 11.05, 11.86 GHz) which are very close to the integer frequency values used before, when the actual thickness is 7 mm. Fig. 5 shows the estimated thickness and permittivity values for different number of observations, N, as explained in section III-D. Increasing the number of observations averages out the noise effect and yields better estimation. For single observation (N=1), the error in the estimation is 1.2 mm. When N increases to 2, 5, and 10, the estimated thickness improves to 7.8, 7.7, and 7.6 mm. The estimated thickness and permittivity converges to 7.65 mm and 2.85 respectively almost after 13 observations. Unfortunately, we are not able to compare the estimated permittivity to the actual value since the latter has not been measured during the in-lab experimental procedure. The results show that the model can correctly estimate the experimental oil thickness even though it was only trained on simulated data and not exposed to any experimental data. This reinforces the effectiveness of our approach for practical use.

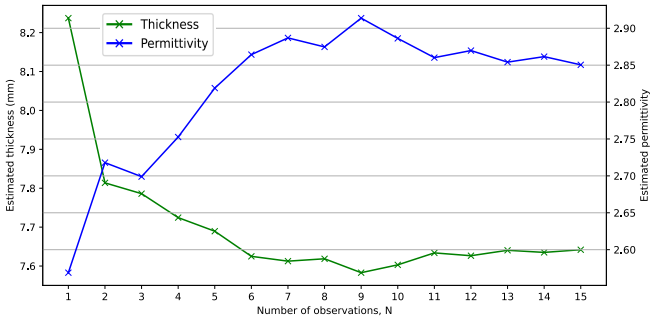

Fig. 5: Estimated thickness and permittivity obtained by the ANN when processing experimental reflectivities while increasing the number of observations.

TABLE I: Complexity of the ANN model on FPGA

	LUT (%)	BRAM (%)	DSP (%)	FF (%)	Power [W]
Rolled	1.88	1.79	1.82	1.13	$3.40{\cdot}10^{-2}$
Unrolled	28.37	1.43	25.91	15.28	$1.33{\cdot}10^{-1}$

VI. FPGA Implementation

Using battery-powered devices like drones as potential platforms, energy and power consumption is of high importance. In contrast, ANNs often introduce high complexity in terms of memory footprint and computational requirements. To show the feasibility of our approach and verify the low-complexity of our ANN, we present in Table I implementation results on the low-cost, low-power Pynq Z1 FPGA. We implement a sequential version of the ANN inference (rolled), using only one processing element for each layer, as well as a fully parallel version by instantiating a processing element for each neuron (unrolled). The results show that only a small fraction of the available resources of the FPGA is utilized by our implementation. This is also reflected in the power consumption which ranges between 34 and 133 mW. As the power drawn by drones is in the order of 10th of Watts, the power consumption of our ANN implementation is negligible. This verifies the feasibility of our ANN-based approach and demonstrated the suitability for a practical scenario.

VII. Conclusion

In this paper, we demonstrate how a simple ANN-based model can be used not only to accurately estimate the thickness of oil slicks, but also to estimate their relative permittivity for classification. This work is a proof-of-concept that active radar sensors data, processed by low-power low-complexity ANNs, can be used as complementary oil-spills monitoring systems for quick intervention. It is a step forward in the oil-spill remote sensing field towards practical solutions. This concept can be further developed by using larger and more complex machine learning models, and with additional more diversified training data of higher quality to achieve better thickness estimations in varied environments.

References

[1] G. M. Barenboim, V. M. Borisov, V. Golosov, and A. Y. Saveca, "New problems and opportunities of oil spill monitoring systems," *Proceedings of the International Association of Hydrological Sciences*, vol. 366, pp. 64–74, 2015.

[2] S. Hook, G. Batley, M. Holloway, A. Ross, and P. Irving, *Oil spill monitoring handbook*. Csiro Publishing, 2016.

[3] Z. H. Shah and Q. Tahir, "Dielectric properties of vegetable oils," *Journal of Scientific Research*, vol. 3, no. 3, pp. 481–492, 2011.

[4] M. Fingas, "How to measure oil thickness (or not)," *AMOP, Environment Canada, Ottawa, Ontario*, pp. 617–652, 2012.

[5] W.-C. Shih and A. B. Andrews, "Infrared contrast of crude-oil-covered water surfaces," *Optics letters*, vol. 33, no. 24, pp. 3019–3021, 2008.

[6] M. FingaS, "The challenges of remotely measuring oil slick thickness," *Remote Sensing*, vol. 10, no. 2, p. 319, 2018.

[7] M. N. Jha, J. Levy, and Y. Gao, "Advances in remote sensing for oil spill disaster management: state-of-the-art sensors technology for oil spill surveillance," *Sensors*, vol. 8, no. 1, pp. 236–255, 2008.

[8] M. Fingas and C. E. Brown, "A review of oil spill remote sensing," *Sensors*, vol. 18, no. 1, p. 91, 2017.

[9] Z. Jiang, J. Zhang, Y. Ma, and X. Mao, "Hyperspectral remote sensing detection of marine oil spills using an adaptive long-term moment estimation optimizer," *Remote Sensing*, vol. 14, no. 1, p. 157, 2022.

[10] Y. Hou, Y. Li, B. Liu, Y. Liu, and T. Wang, "Design and implementation of a coastal-mounted sensor for oil film detection on seawater," *Sensors*, vol. 18, no. 1, p. 70, 2018.

[11] C. C. Texeira, C. Y. S. Siqueira, F. R. A. Neto, F. P. Miranda, J. R. Cerqueira, A. O. Vasconcelos, L. Landau, M. Herrera, and K. Bannermaman, "Source identification of sea surface oil with geochemical data in cantarell, mexico," *Microchemical Journal*, vol. 117, pp. 202–213, 2014.

[12] Y. Li, Q. Yu, M. Xie, Z. Zhang, Z. Ma, and K. Cao, "Identifying oil spill types based on remotely sensed reflectance spectra and multiple machine learning algorithms," *IEEE Journal of Selected Topics in Applied Earth Observations and Remote Sensing*, vol. 14, pp. 9071–9078, 2021.

[13] A.-B. Salberg and S. Ø. Larsen, "Classification of ocean surface slicks in simulated hybrid-polarimetric sar data," *IEEE Transactions on Geoscience and Remote Sensing*, vol. 56, no. 12, pp. 7062–7073, 2018.

[14] G. Daou, C. B. Maroun, and B. Hammoud, "Advanced iterative multi-frequency algorithm used by radar remote-sensing systems for oil-spill thickness estimation," in *2021 International Conference on Electrical, Computer and Energy Technologies (ICECET)*, pp. 1–6, IEEE, 2021.

[15] B. Hammoud, H. Ayad, M. Fadlallah, J. Jomaah, F. Ndagijimana, and G. Faour, "Oil thickness estimation using single-and dual-frequency maximum-likelihood approach," in *2018 International Conference on High Performance Computing & Simulation (HPCS)*, pp. 65–68, IEEE, 2018.

[16] B. Hammoud, G. Daou, and N. Wehn, "Multidimensional minimum euclidean distance approach using radar reflectivities for oil slick thickness estimation," *Sensors*, vol. 22, no. 4, p. 1431, 2022.

[17] C. B. Maroun, G. Daou, B. Hammoud, and B. Hammoud, "Machine learning using support vector regression in radar remote sensing for oil-spill thickness estimation," in *2021 18th European Radar Conference (EuRAD)*, pp. 221–224, IEEE, 2022.

[18] B. Hammoud, F. Mazeh, K. Jomaa, H. Ayad, F. Ndadijimana, G. Faour, M. Fadlallah, and J. Jomaah, "Multi-frequency approach for oil spill remote sensing detection," in *High Performance Computing & Simulation (HPCS), 2017 International Conference on*, pp. 295–299, IEEE, 2017.

[19] F. T. Ulaby, D. G. Long, W. J. Blackwell, C. Elachi, A. K. Fung, C. Ruf, K. Sarabandi, H. A. Zebker, and J. Van Zyl, *Microwave radar and radiometric remote sensing*, vol. 4. University of Michigan Press Ann Arbor, 2014.

[20] G. De Carolis, M. Adamo, and G. Pasquariello, "On the estimation of thickness of marine oil slicks from sun-glittered, near-infrared meris and modis imagery: the lebanon oil spill case study," *IEEE Transactions on Geoscience and Remote Sensing*, vol. 52, no. 1, pp. 559–573, 2013.

[21] B. Hammoud, K. Jomaa, F. Ndagijimana, G. Faour, H. Ayad, and J. Jomaah, "Experimental validation of algorithms used by radar remote-sensing systems for oil-spill detection and thickness estimation," in *2019 16th European Radar Conference (EuRAD)*, pp. 205–208, IEEE, 2019.